Available online at www.sciencedirect.com
ScienceDirect
Journal of Molecular Graphics and Modelling 26 (2008) 1213–1222
Journal of Molecular Graphics and Modelling
www.elsevier.com/locate/JMGM

Molecular docking/dynamics studies of Aurora A kinase inhibitors

Tanaji T. Talele [a,*], Mark L. McLaughlin [b,c,*]

[a] Department of Pharmaceutical Sciences, College of Pharmacy and Allied Health Professions, St. John's University, Jamaica, NY 11439, United States
[b] Department of Chemistry, University of South Florida, Tampa, FL 33620, United States
[c] Drug Discovery Program, H. Lee Moffitt Cancer Center and Research Institute, 12902 Magnolia Drive, MRC 4 East, Tampa, FL 33612, United States

Received 24 May 2007; received in revised form 3 November 2007; accepted 3 November 2007
Available online 17 November 2007

Abstract

The binding modes of a known 1,4,5,6-tetrahydropyrrolo[3,4-*c*]pyrazole, quinazoline, pyrimidine and indolinone series of Aurora A kinase inhibitors have been studied using molecular docking and molecular dynamics (MD) simulations. Crystallographic bound compound **8** was precisely predicted by our docking procedure as evident from 0.43 Å root mean square (rms) deviations. In addition compound **25** (AZ_68) has been successfully cross-docked within the Aurora A kinase active site, which was pre-organized for inhibitor **8**. We found four key sites (A: solvent-exposed front pocket, B: hinge region, C: selectivity pocket and D: solvent-exposed phosphate binding region) of the Aurora A kinase contributing towards the binding of these compounds. We suggest that the small hydrophobic substituents at C-6 position of pyrrolopyrazole nucleus (in compounds **1**–**8**); C-6 and C-7 positions of the quinazoline moiety (in compounds **9**–**23**); C-2 position of the quinazoline and C-4 position of the pyrimidine (in compound **25**) could be more effective and selective through increased hydrophobic contacts and selectivity pocket interactions with these modifications of Aurora A kinase inhibitors. Five representative complexes were subjected to 1000 ps of MD simulation to determine the stability of the predicted binding conformations. The low value of the root mean square deviations (ranging from 0.725 to 1.820 Å) between the starting complex structure and the energy minimized final average complex structure suggests that the Glide Extra Precision (XP) derived docked complexes are in a state of near equilibrium. The structure-based drug design strategy described in this study will be highly useful for the development of new inhibitors with high potency and selectivity.

Keywords: Aurora A kinase; Docking; Molecular dynamics simulation

1. Introduction

One of the emerging targets in oncology drug discovery is the Aurora kinases [1], a small family composed of three Ser/Thr protein kinases: Aurora A–C. At least two of the Aurora kinases (Aurora A and B) are commonly overexpressed in human tumors including breast, lung, colon, ovarian and pancreatic cancers [2–4]. Overexpression of Aurora A leads to centrosome amplification and aneuploidy, and has also been shown to compromise spindle checkpoint function, allowing anaphase to occur despite continued activation of the checkpoint [5,6]. Furthermore Aurora A has been shown to function as an oncogene [7,8]. Recent clinical experience and subsequent approvals of small-molecule kinase inhibitors such as Imatinib [9], Gefitinib [10] and Erlotinib [10] illustrate the tractable nature of this class of enzymes for the development of anticancer drugs. Encouragingly, VX-680 (MK-0457) discovered at Vertex Pharmaceuticals, is a potent and selective inhibitor of Aurora kinases and it just recently progressed into phase II clinical development [11].

It has been recognized that highly specific ATP-competitive inhibitors can be obtained against a number of different kinases with clinical uses as cancer therapeutic agents [12]. Understanding the molecular constraints of the ATP-binding site of Aurora A kinase and the structural basis for its interactions with ATP and ATP-competitive inhibitors is an essential step in designing inhibitors for this subfamily of kinases that are both selective and potent. In conjunction with our efforts to design and synthesize potent and selective Aurora A kinase inhibitors,

* Corresponding authors.
E-mail addresses: talelet@stjohns.edu (T.T. Talele), mmclaugh@chuma1.cas.usf.edu (M.L. McLaughlin).

1093-3263/$ – see front matter © 2007 Elsevier Inc. All rights reserved.
doi:10.1016/j.jmgm.2007.11.003

Table 1
Chemical structures of compounds **1–28** that were docked to the ATP-binding site of the Aurora A kinase along with biological activity and binding energy data[a]

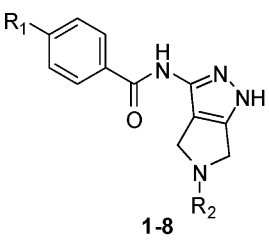

1-8

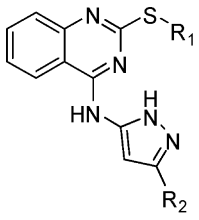

9-16,18-23

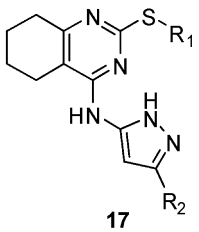

17

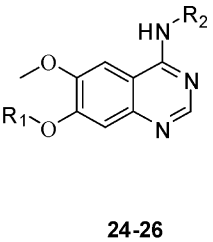

24-26

Compounds	R_1	R_2	Binding energy		Compounds **1–8**, **24–26**, **28** IC_{50} compounds **9–23**, **27**, K_i (nM)
			Gscore[b]	Emodel[b]	
1	*tert*-Butyl	2-(Thiophen-2-yl)acetyl	−14.76	−77.58	5.0
2	*tert*-Butyl	2-Furoyl	−14.12	−70.95	41.0
3	*tert*-Butyl	2-Phenylacetyl	−13.49	−73.31	130.0
4	*tert*-Butyl	–C(=O)–NH–2,6-diethylphenyl	−14.53	−85.66	100.0
5	*N*-Methylpiperazine	2-(Thiophen-2-yl)acetyl	−14.93	−79.58	65.0
6	*N*-Methylpiperazine	2-Furoyl	−13.91	−72.83	160.0
7	*N*-Methylpiperazine	2-Phenylacetyl	−14.83	−73.51	140.0
8	N-methylpiperazine	–C(=O)–NH–2,6-diethylphenyl	−14.81	−91.10	27.0
9	Phenyl	$–CH_3$	−7.19	−60.66	<100
10	4-Methoxyphenyl	$–CH_3$	−7.34	−64.53	<100
11	2,4-bis(Trifluoromethyl)phenyl	$–CH_3$	−6.31	−64.50	<100
12	1-Methyl-1H-imidazol-2-yl	$–CH_3$	−5.89	−60.14	<100
13	Naphthalen-2-yl	$–CH_3$	−10.42	−66.55	<100
14	Benzimidazol-2-yl	$–CH_3$	−7.41	−60.44	<100
15	Phenyl	–Cyclopropyl	−6.57	−63.23	<100
16	Naphthalen-2-yl	–Cyclopropyl	−6.03	−69.06	<100
17	Naphthalen-2-yl	–Cyclopropyl	−5.93	−62.47	<100
18	Benzimidazol-2-yl	–Cyclopropyl	−7.45	−61.88	<100
19	Naphthalen-1-yl	–Cyclopropyl	−7.43	−68.68	<100
20	4-Acetamidophenyl	–Cyclopropyl	−7.67	−72.72	<100
21	4-Acetamidophenyl	$–CH_3$	−7.43	−71.05	<100
22	4-Methylsulfonamidophenyl	$–CH_3$	−7.81	−69.52	<100
23	4-Isopropylsulfonamidophenyl	$–CH_3$	−7.30	−73.37	<100
24	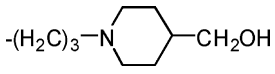	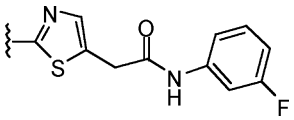	−9.27	−88.65	<1.0
25	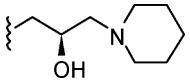	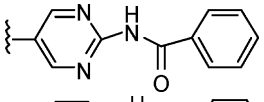	−9.98	−85.76	6.0
26	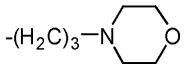	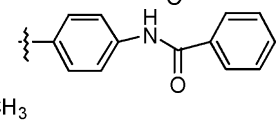	−9.10	−74.43	110.0
27	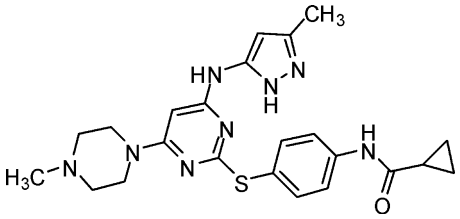		−8.62	−67.72	0.0006
28	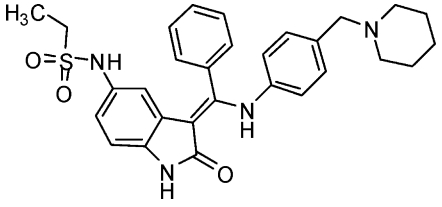		−11.60	−87.91	250.0 (Aurora B)

[a] A more negative Gscore (Glide score) indicates a better fit in the binding site.
[b] Gscore and Emodel are expressed as kcal/mol.

we first carried out a structure-based molecular modeling study on the recently deposited X-ray structure of Aurora A kinase in complex with compound **8** [13]. To the best of our knowledge, this is the first report on the prediction of binding modes of recently published Aurora A kinase inhibitors.

2. Materials and methods

2.1. Biological data

The Aurora A kinase inhibitory activity of 28 tetrahydropyrrolo[3,4-*c*]pyrazole, quinazoline, pyrimidine and indolinone derivatives, which were measured *in vitro* as the IC_{50} or K_i values were taken from literature [11,13–18]. The structures of these inhibitors along with binding energy and biological activity are shown in Table 1.

2.2. Ligand structure preparation

All the compounds were constructed using the fragment dictionary of Maestro 7.5 and geometry optimized by Macromodel program v9.1 (Schrodinger, LLC) using the Optimized Potentials for Liquid Simulations-all atom (OPLS-AA) force field [19] with the steepest descent followed by truncated Newton conjugate gradient protocol. Partial atomic charges were computed using the OPLS-AA force field.

2.3. Protein structure preparation

The X-ray crystal structure of Aurora A kinase in complex with compound **8** (PDB ID: 2BMC) obtained from the RCSB Protein Data Bank (PDB) was used in order to model the protein structure in this study. Water molecules of crystallization were removed from the complex, and the protein was optimized for docking using the protein preparation and refinement utility provided by Schrödinger LLC and the Impact program (FirstDiscovery v4.0). Partial atomic charges were assigned according to the OPLS-AA force field.

2.4. Docking protocol

All docking calculations were performed using the ''Extra Precision'' (XP) mode of Glide program (FirstDiscovery v4.0) and the 2001 implementation of the OPLS-AA force field. Although details on the methodology used by Glide are described elsewhere [20–23], a short description is provided below. The binding site, for which the various energy grids were calculated and stored, is defined in terms of two concentric cubes: the bounding box, which must contain the center of any acceptable ligand pose, and the enclosing box, which must contain all ligand atoms of an acceptable pose. Cubes with an edge length of 12 Å and centered at the midpoint of the longest atom–atom distance in the respective cocrystallized ligand defined the bounding box in the protein. The larger enclosing box was also defined in terms of the cocrystallized ligand: an edge length of 30 Å was used. Poses with an rmsd of less than 0.5 Å and a maximum atomic displacement of less than 1.3 Å were eliminated as redundant in order to increase diversity in the retained ligand poses. The scale factor for van der Waals radii was applied to those atoms with absolute partial charges less than or equal to 0.15 (scale factor of 0.8) and 0.25 (scale factor of 1.0) electrons for ligand and protein, respectively. The *maxkeep* variable which sets the maximum number of poses generated during the initial phase of the docking calculation were set to 5000 and the *keep best* variable which sets the number of poses per ligand that enters the energy minimization was set to 1000. Energy minimization protocol includes dielectric constant of 4.0 and 1000 steps of conjugate gradient. Upon completion of each docking calculation, at most 100 poses per ligand were generated. The best docked structure was chosen using a Glidescore (Gscore) function. The Gscore is a modified and extended version of the empirically based Chemscore function [24]. Another scoring function used by Glide is Emodel, which itself derived from a combination of the Gscore, Coulombic, van der Waals and the strain energy of the ligand. All computations were carried out on a Dell Precision 470n dual processor with the Linux OS (Red Hat Enterprise WS 4.0).

2.5. Molecular dynamic (MD) simulations

MD simulations were carried out on energy-minimized Aurora A kinase-representative inhibitor docked whole complex using Impact 4.0 (Schrodinger, LLC) with the OPLS-AA force field and a generalized Born/solvent-accessible surface area (GB/SA) implicit water solvent model with a dielectric constant of 78. The complex was subjected to 1000 ps MD simulations at 300 K with an integration step of 1 fs and NVT as an ensemble type. All covalent bonds containing the hydrogen atoms were constrained using SHAKE algorithm, with a tolerance of 10^{-7} Å. System coordinates were saved every 2 ps for further analysis. Three-dimensional structures and trajectories were visually inspected using the Maestro graphical interface. Root mean square (rms) deviations from the initial structures were calculated using superposition option in Maestro. An average structure obtained from the last 500 ps of MD simulations was refined by means of 1000 steps of steepest descent followed by conjugate gradient energy minimization. Conjugate gradient energy minimizations were performed four times using the positional restraints to all heavy atoms with 1000, 500, 100 and 0 kJ/mol $Å^2$ force constants in sequence. The maximum number of cycles of minimization was 5000 and the convergence criterion for the energy gradient was 0.001 kJ/mol Å.

3. Results and discussion

3.1. Validation of the docking protocol

The most straightforward method of evaluating the accuracy of a docking procedure is to determine how closely the lowest energy pose (binding conformation) predicted by the object scoring function, Glidescore (Gscore) in our case, resembles an experimental binding mode as determined by X-ray crystal-

lography. In the present study, Extra Precision Glide docking procedure was validated by removing compound **8** from the binding site and redocking it to the binding site of Aurora A kinase. We found a very good agreement between the localization of the inhibitor upon docking and from the crystal structure, i.e. having similar hydrogen bonding interactions with Glu211 and Ala213. Interestingly our docking procedure also uncovered an additional hydrogen bonding interaction with Lys162. The root mean square deviations between the predicted conformation and the observed X-ray crystallographic conformation of compound **8** equaled 0.43 Å, a value that suggests the reliability of Glide docking in reproducing the experimentally observed binding mode for Aurora A kinase inhibitor and the parameter set for the Glide docking is reasonable to reproduce the X-ray structure (Fig. 1a).

3.2. Cross docking of compound 25 (AZ_68) in compound 8 bound active site of Aurora A kinase

Cross docking involves the docking of a ligand to a receptor complexed with another compound (i.e. to active site pre-organized for another compound) and thus provides a rigorous validation of the docking protocol. Accordingly compound **25** was docked within the active site (pre-organized for compound **8**) of Aurora A kinase using Extra Precision Glide method. We found a very good agreement between the localization of the compound **25** from docking and from the crystal structure (PDB ID: 2C6E) [16] as evidenced by <1.00 Å rms deviations. Consequently, the Glide docking method is a highly reliable means of reproducing the experimentally observed binding mode for Aurora A kinase inhibitor.

3.3. Architecture of the Aurora A kinase binding site

The ATP-binding pocket of Aurora A kinase is considerably hydrophobic and has several key sites of interest for the design of new Aurora A kinase inhibitors. The molecular superposition of bound conformations of representative compounds from each series indicates that these compounds have more or less identical binding mode with Aurora A kinase, especially for the hinge region and the highly solvent-exposed phosphate binding region (Fig. 1b). Four key sites A–D on the surface binding groove of Aurora A kinase are also indicated in Fig. 1b. Site A is the solvent-exposed front pocket formed by Tyr212, Ala213, Pro214, Leu215, Gly216, Arg220, Lys224, Leu264, Gly265, Ser266, Arg137, Leu139, and Phe157 amino acid residues. Site B is the hinge region (formed by 210–216 amino acid residues) where pyrazole, quinazoline and other nitrogen rich heterocycles having hydrogen bond donor/acceptor functionalities are preferred. This site is mainly focused on H-bonding network. The 6-amino and 1-imido groups of adenosine bind to the hinge region of the Aurora A kinase active site through direct hydrogen bonds with the main chain amides of residues Glu211 and Ala213. Site C is referred as the selectivity pocket (hydrophobic back pocket). This site is present in most of the kinases and is created by residues Leu210 and Glu211 (in the hinge region), Val147 (in the glycine-rich loop), and Ala160

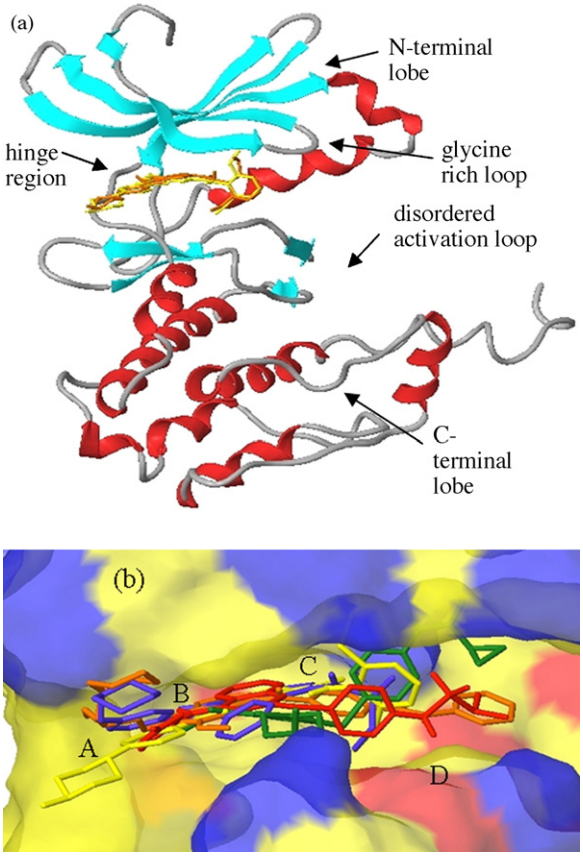

Fig. 1. (a) Conformational comparison of compound 8 from the crystal structure of compound **8**–Aurora A kinase (2BMC) complex (orange) and that predicted by XPGlide (yellow) are shown within the active site of Aurora A kinase. Protein backbone atoms are depicted by ribbons. (b) XPGlide-predicted pose for representative compounds from each series: compounds **8** (yellow), **23** (red), **25** (orange), **27** (green) and **28** (violet) resulting from molecular docking and their superposition in the ATP-binding site of Aurora A kinase. Four key sites (A–D) contributing for the binding of these compounds are also shown. Aurora A kinase is represented as Macromodel surface according to residue charge (electropositive charge: blue, electronegative charge: red, neutral: yellow) as implemented in Maestro. (For interpretation of the references to color in this figure legend, the reader is referred to the web version of the article.)

and Leu194 in Aurora A kinase. The hydrophobic back pocket is not conserved and is used to gain affinity as well as selectivity. Access to this pocket is controlled by a gatekeeper amino acid residue (Leu210 in case of Aurora A kinase). Site D is a highly solvent-exposed phosphate binding region which is relatively larger compared to the solvent-exposed front pocket (site A) and is formed by the amino acid residues Lys143, Phe144, Lys162, Leu164, Leu178, Glu181, Leu194, Leu208, Arg255, Lys258, Glu260, Asn261, Leu263, Lys271, Ile272, Ala273, Asp274, Phe275, and Trp277.

The structural analysis described above suggests that the highly solvent-exposed sites A and D could be exploited to improve the pharmacokinetic properties of lead compounds since these sites are located outside the ATP-binding site.

3.4. Docking studies

A group of 28 compounds reported to inhibit Aurora A kinase (except compound **28**, which is an Aurora B kinase

inhibitor) were chosen from the recent literature [11,13–18] to investigate their binding mode within the active site of Aurora A kinase. Automated docking of compounds **1**–**28** was carried out without explicit active site water molecules and in each docking calculation a maximum of 100 poses were saved. After the graphical analysis of the Aurora A kinase-inhibitor complexes, the same ligand conformation and relative orientation for each series were selected. On the basis of the nature of their central heterocycle and of their substitution pattern, these compounds can be divided into five classes: pyrrolopyrazole (compounds **1**–**8**); 2,4-disubstituted quinazoline (compounds **9**–**23**); 4,6,7-trisubstituted quinazoline (compounds **24**–**26**); 2,4,6-trisubstituted pyrimidine (compound **27** or VX-680) and indolinone (compound **28** or Hesperadin) derivatives. The predicted binding affinity of these compounds is shown in Table 1.

*3.4.1. Binding mode of 1,4,5,6-tetrahydropyrrolo[3,4-c]pyrazole derivatives (compounds **1**–**8**)*

A comparison of the different docking poses of compounds **1**–**8** suggests that these compounds adopt similar binding modes with the H-bonding network. To illustrate the binding mode of this series of compounds, compound **8**, one of the potent Aurora A kinase inhibitors, was analyzed in more detail. Fig. 2a shows a docked model of compound **8** into the active site of Aurora A kinase. The tetrahydropyrrolo[3,4-*c*]pyrazole ring binds in a deep catalytic active site formed by the hinge region (residues 210–216) through three hydrogen bonds. Pyrazole –N– and –NH ring atoms form hydrogen bonds with Ala213 (–N···HN, $d_2 = 2.07$ Å, $\theta_2 = 177.5^\circ$) and Glu211 (–NH···O, $d_3 = 1.84$ Å, $\theta_3 = 154.6^\circ$) backbone, respectively. The 3-amino function of the tetrahydropyrrolo[3,4-*c*]pyrazole ring forms a hydrogen bond with the backbone Ala213 (–NH···O, $d_1 = 2.41$ Å, $\theta_1 = 139.1^\circ$). The carbonyl oxygen at the N-5 position forms a hydrogen bond with the Lys162 side chain (O···H_2N, $d_4 = 1.88$ Å, $\theta_4 = 161.7^\circ$) located in the upper lobe of the highly solvent-exposed phosphate binding site of Aurora A kinase. Further stabilization of the binding was mediated by the contact of the *N*-methylpiperazinylbenzoyl moiety with the hydrophobic surface formed by Leu139, Tyr212, Pro214, Leu215, and Leu263 amino acid side chains. This moiety is located in the solvent-exposed front pocket of the Aurora A kinase. Being exposed to the solvent, this moiety offers a good handle for improving the pharmacokinetic profile through chemical modification. The 2,6-diethylaniline group was found to interact with a hydrophobic surface formed by Val147, Lys162, Lys141, Ala273 and Leu164 residues found in the vicinity of a highly solvent-exposed phosphate binding site. On the basis of the docked geometry, it appears that compounds **1**–**8** assume a v-shape conformation within the active site of Aurora A kinase.

*3.4.2. Binding mode of 2,4-disubstituted quinazoline derivatives (compounds **9**–**23**)*

A comparison of different docking poses of compounds **9**–**23** suggests that they bind to Aurora A kinase in a same manner. To illustrate the binding mode of this series of compounds,

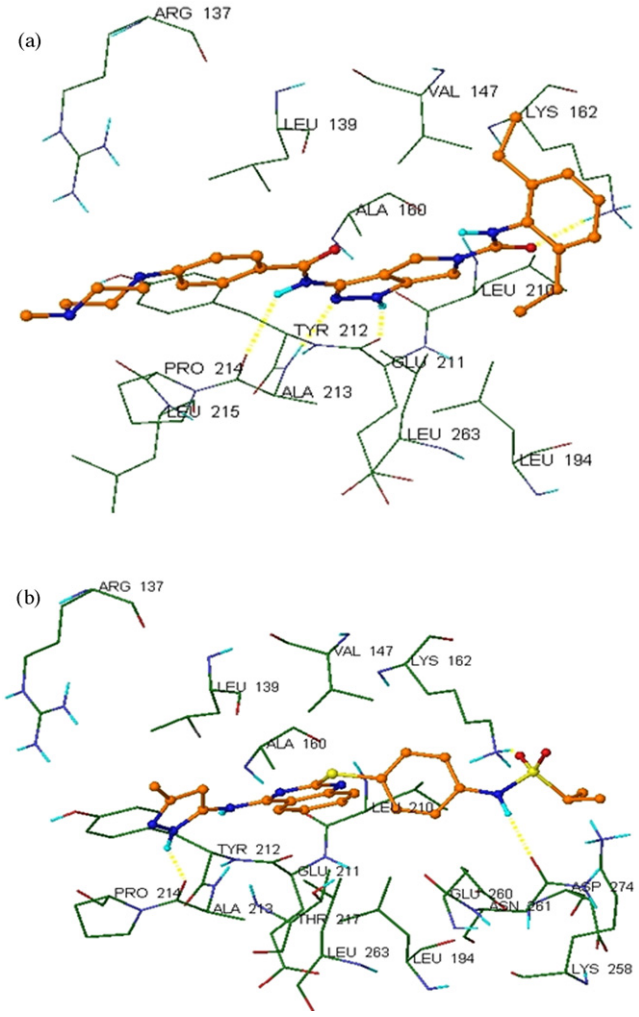

Fig. 2. XPGlide-predicted pose for compounds 8 (panel a) and **23** (panel b) with the Aurora A kinase active site. For clarity, only the polar hydrogens are shown. Hydrogen bonds are shown as dotted yellow lines. Active site amino acid residues are represented as sticks with the atoms colored as carbon: green, hydrogen: cyan, nitrogen: blue, oxygen: red and sulfur: yellow) while the inhibitor is shown as ball and stick model with same color scheme as above except carbons are represented in orange. (For interpretation of the references to color in this figure legend, the reader is referred to the web version of the article.)

compound **23** was selected for more detailed analysis. Fig. 2b shows the docked model of compound **23** within the active site of Aurora A kinase. The pyrazole ring –NH interacts through hydrogen bonding with the backbone of Ala213 amino acid residue (–NH···O, 2.08 Å, 149.2°) in the hinge region. The 3-amino function of pyrazole was found to be 3.17 Å away from the backbone carbonyl oxygen of Ala213. The quinazoline ring binds near the hinge region and forms hydrophobic contacts with Leu139, Val147, Ala160, Leu194, Leu210, Tyr212, Ala213 and Leu263. The phenyl part of the quinazoline nucleus was found to bind to the inside of the selectivity pocket. The pyrazole ring is located in the solvent-exposed front pocket where it interacts with Arg137, Leu139, Tyr212 and Pro214.

It is worthwhile to note that 5-methyl/cyclopropyl substituent on the pyrazole ring of compounds in this series is located near the side chain of Arg137, thus suggesting that the

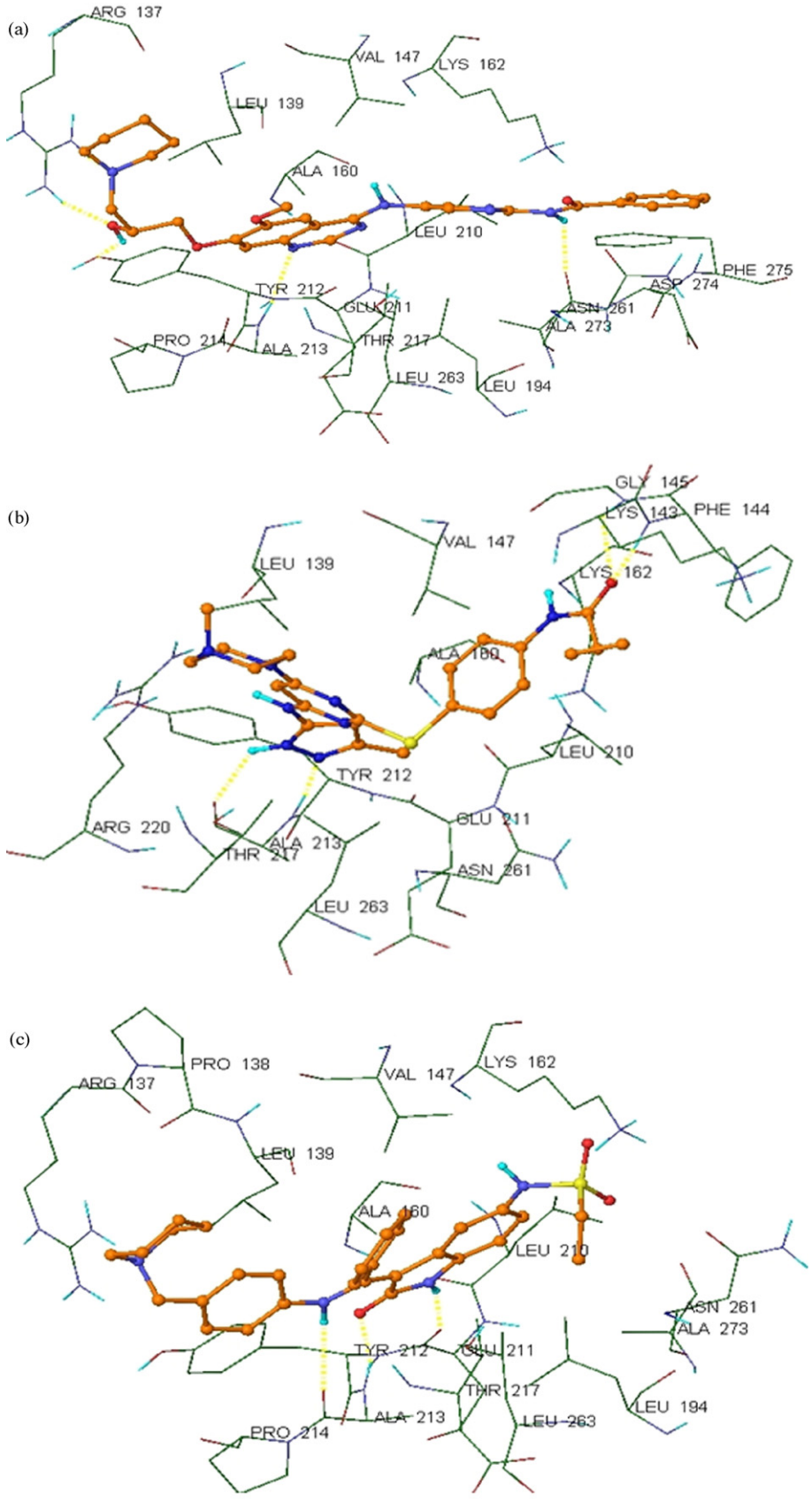

Fig. 3. XPGlide-predicted pose for representative compounds 25 (panel a), **27** (panel b), and **28** (panel c) with the Aurora A kinase active site. For clarity, only the polar hydrogens are shown. Hydrogen bonds are shown as dotted yellow lines. Active site amino acid residues are represented as sticks with the atoms colored as carbon: green, hydrogen: cyan, nitrogen: blue, oxygen: red and sulfur: yellow) while the inhibitor is shown as ball and stick model with same color scheme as above except carbons are represented in orange. (For interpretation of the references to color in this figure legend, the reader is referred to the web version of the article.)

introduction of a chemical modification at this site in the form of a carboxylate or a tetrazole group to enhance the interaction of the inhibitor with Aurora A kinase through a salt bridge. This kind of salt bridge interaction for increasing the binding affinity of the lead compound has been recently proved by experiment [25]. The arylthio moiety is located in the highly solvent-exposed phosphate binding site where it forms hydrophobic interactions with Phe144, Val147, Lys162, Thr217, Lys258, Glu260, Asn261 and Asp274. The oxygen atom and –NH function of the sulfonamide group in the phosphate-binding region is involved in hydrogen bonding network with Lys162 (O···HN, 2.03 Å, 154.8°) and Asn261 (–NH···O, 2.11 Å, 167.0°) side chains, respectively. Overall it is verified that the arylthio moiety, pyrazole ring and quinazoline ring prefer to position themselves near the highly solvent-exposed phosphate binding site, the solvent-exposed front pocket and the hinge region, respectively.

3.4.3. Binding mode of 4,6,7-trisubstituted quinazoline derivatives (compounds **24–26**)

A comparison of different docking poses of compounds **24–26** suggests that although they bind to Aurora A kinase in a similar manner, they do it through a different H-bonding network. Fig. 3a shows the docked model of compound **25** within the active site of Aurora A kinase. The predicted binding mode of compound **25** was similar to that found by X-ray crystallography (successful cross-docking as described above) [16]. The quinazoline ring binds near the hinge region and forms hydrophobic contacts with Leu139, Val147, Ala160, Leu194, Leu210, Tyr212 and Ala213 amino acid residues. The N-1 atom of the quinazoline ring forms hydrogen bond with Ala213 backbone (N···HN, 2.46 Å, 171°). The 6-methoxy group on the quinazoline ring forms hydrophobic contacts with the side chains of Thr217 and Leu263. The 7-substituent of the quinazoline ring binds to the solvent-exposed front pocket where it interacts with Arg137, Leu139, Tyr212 and Pro214 amino acid residues. The piperidine ring nitrogen enters in hydrogen bonding interaction with the guanidine group of Arg137 (N···H_2N, 2.09 Å, 149.2°). The 2-hydroxyl group of propoxy moiety forms hydrogen bonds with the side chains of residues Arg137 (O···H_2N, 2.09 Å, 162.2°) and Tyr212 (–OH···O, 2.34 Å, 130.2°). The 2-benzamidopyrimidinyl moiety is located in the highly solvent-exposed phosphate binding site where it forms hydrophobic interactions with residues Phe144, Val147, Lys162, Thr217, Lys258, Glu260, Asn261, Ala273, Asp274 and Phe275. The pyrimidine nitrogen and benzamido carbonyl oxygen atoms are located within H-bonding distance (2.14 and 3.79 Å, respectively) from the side chain of Lys162. Likewise, MD simulations revealed the Lys162 residue to enter in hydrogen bonding with the benzamido carbonyl oxygen. The –NH group of benzamido moiety forms hydrogen bond with the backbone of Ala273 (–NH···O, 2.27 Å, 131.8°).

For compound **24** (AZ_46), the N-1 atom of the quinazoline ring is 3.09 Å away from the backbone –NH of Ala213. The hydroxyl group of the 4-hydroxymethylpiperidine moiety forms a hydrogen bond with the carbonyl function of backbone of the Pro138 (–OH···O, 2.13 Å, 163.7°). The carbonyl oxygen and –NH of the thiazolylacetamide form hydrogen bonds with the side chains of Lys162 (O···H_2N, 1.93 Å, 137.6°) and Asn261 (–NH···O, 2.04 Å, 160.0°), respectively.

For compound **26** (ZM447439), the N-1 atom of the quinazoline ring is 3.26 Å away from the backbone –NH of Ala213. The 4-amino function of the quinazoline ring forms hydrogen bond with Leu139 backbone (–NH···O, 2.33 Å, 151.6°). The carbonyl oxygen atom of the benzamido moiety is located within hydrogen bonding distance (2.50 Å) from Lys162 side chain amino function. The morpholine ring N and O atoms were also found to be within hydrogen bonding distances (2.63 and 2.66 Å) from the guanidino group of Arg137, respectively.

3.4.4. Binding mode of compound **27** (VX-680)

Fig. 3b shows docked model of compound **27** within the active site of Aurora A kinase. The pyrazole ring –N and –NH atoms form hydrogen bond with the backbone atoms of Ala213 (N···HN, 2.19 Å, 162.6° and NH···O, 2.36 Å, 129.1°), respectively. The carbonyl oxygen atom of cyclopropanecarboxamide moiety forms hydrogen bonds with the backbone atoms of Phe144 (O···HN, 1.81 Å, 140.2°) and Gly145 (O···HN, 2.39 Å, 124.5°), respectively. The pyrimidine ring forms hydrophobic contacts with Thr217, Leu263, Leu139 and Gly140 amino acid residues. The piperazine moiety binds in the solvent-exposed front pocket where it interacts with Arg220 and Thr217 side chains. The cyclopropylcarboxamidophenylthio moiety is located in the highly solvent-exposed phosphate binding site where it interacts with the amino acid residues Val147, Lys162, Gly142, Lys143, Phe144, Gly145 and Asn261.

3.4.5. Binding mode of compound **28** (Hesperadin)

Fig. 3c shows docked model of compound **28** within the active site of Aurora A kinase. The predicted conformation and hydrogen bonding network of compound **28** in the active site of Aurora A kinase was similar to that of experimental structure of the same compound in complex with Aurora B kinase [26]. The indolinone moiety binds near the hinge region and forms hydrophobic contacts with Val147, Ala160, Leu194, Leu210, Tyr212 and Ala213 amino acid residues. The carbonyl oxygen and –NH atoms of indolinone ring form hydrogen bonds with Ala213 (O···HN, 1.82 Å, 159.0°) and Glu211 (–NH···O, 2.28 Å, 157.9°) backbone atoms, respectively. The central phenyl ring of benzylidene moiety makes hydrophobic contacts with Gly216, Thr217 and Leu263 amino acid residues. The piperidine moiety binds in the solvent-exposed front pocket where it interacts with Arg137, Pro138, Leu139, Tyr212, Pro214 and Gly216 amino acid residues. The aniline –NH forms hydrogen bond with Ala213 backbone (–NH···O, 2.37 Å, 133.2°). The ethylsulfonamide moiety binds in the highly solvent-exposed phosphate binding site where it interacts with Lys162, Thr217, Glu260, Asn261, Leu263 and Ala273 amino acid residues. The sulfonamide oxygen atoms are located within hydrogen bonding distances (2.07 and 2.64 Å) from that of Lys162 side chain amino function. Indeed this hydrogen bonding interaction exists as evidenced by MD simulations.

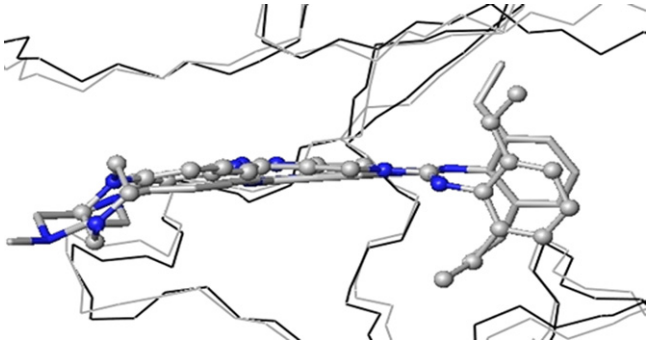

Fig. 4. View of superimposed backbone atoms of the energy-minimized average structure of the last 500 ps of the MD simulation (black) and the initial structure (gray) for compound 8–Aurora A kinase complex. Compound **8** is represented in stick for initial complex and ball/stick for the final average complex.

3.5. MD simulations

To take into account protein flexibility, the behavior of the predicted complex was studied in a dynamic context. The superposition of coordinates of each complex structure in a trajectory (500 structures) onto the initial structure allowed us to analyze the progression of the root mean square deviations. A superposition of the energy minimized average structure and the initial structure of compound **8**–Aurora A kinase complex is shown in Fig. 4. The superposition of the coordinates of energy minimized average structure of compounds **8**, **23**, **25**, **27**, and **28**–Aurora A kinase complex obtained from the last 250 trajectories onto their respective starting complex provided rmsd ranging from 0.725 to 1.820 Å for ligand atom-based superposition. It is interesting to note that the averaging of last 250 trajectories was a necessary step as the minimized docked pose for the representative inhibitors was found to be significantly different compared to the minimized 500 and 1000 ps poses. Furthermore, the stability of the hydrogen bonding network predicted by Glide XP docking method was examined by monitoring the percentage occurrence of predicted hydrogen bonds during the simulation time. The analyses of the MD trajectories of representative inhibitors indicate the presence of several hydrogen bonds between the inhibitors and Aurora A kinase with moderate to high frequencies.

Among the four hydrogen bonds (pyrazole ring NH···CO Glu211, pyrazole ring N···NH Ala213, 3-NH···CO Ala213, and N_5 CO···NH_2 Lys162) in the compound **8**–Aurora A kinase complex, only three were preserved in one third of the MD trajectory. The 3-NH···CO Ala213 hydrogen bond appeared only in ∼10% of the trajectory. All the predicted hydrogen bonds were restored in the energy-minimized average structure of the complex. The results of MD simulation of compound **8**–Aurora A kinase complex are graphically shown in Fig. 5a–c. The initial potential energy was sufficiently low, indicates that the starting structure was well minimized. During the thermalization phase the initial potential energy rapidly increased as kinetic energy was added to the system. After approximately 100 ps all the potential energy curves reached steady-state values as shown in Fig. 5a. The variations of hydrogen bond distances (d_1, d_2, d_3, and d_4) and angles (θ_1, θ_2, θ_3, and θ_4) for compound **8**–Aurora A kinase complex is presented in Fig. 5b and c, respectively. For the identification of hydrogen bonds, distance (H···A) cutoff of about 2.5 Å and

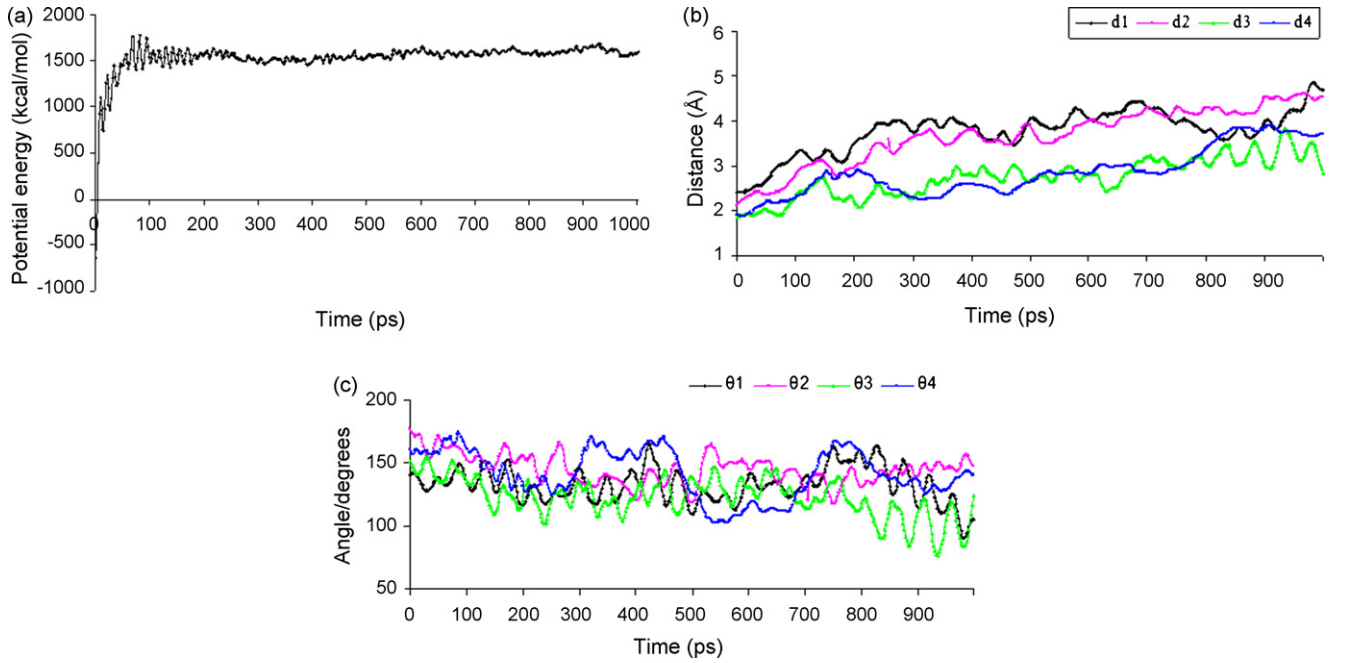

Fig. 5. A trajectory for the compound 8–Aurora A kinase system plotted as a function of simulation time. (a) The potential energy of the compound **8**–Aurora A kinase system, (b) hydrogen bond (H–A) distances (–NH···O Ala213, d_1 = 2.41 Å), (–N···HN Ala213, d_2 = 2.07 Å), (–NH···O Glu211, d_3 = 1.84 Å), and (O···H_2N Lys162, d_4 = 1.88 Å) and (c) hydrogen bond (D–H–A) angles (–NH···O Ala213, θ_1 = 139.1°), (–N···HN Ala213, θ_2 = 177.5°), (–NH···O Glu211, θ_3 = 154.6°), and (O···H_2N Lys162, θ_4 = 161.7°).

angle (D–H–A) >120° were used. Thus a strong hydrogen bond should have an H···A distance of about 2.5 Å and D–H–A angle of >120°. According to these criteria two (–NH···O Glu211) and (O···H_2N Lys162) out of four hydrogen bonds are strong whereas remaining two (–NH···O Ala213) and (–N···HN Ala213) can be considered as transient ones and may be involved in strong electrostatic interactions. The average hydrogen bond distances (d_1 = 3.77 Å, d_2 = 3.66 Å, d_3 = 2.75 Å, and d_4 = 2.84 Å) and angles (θ_1 = 132.9°, θ_2 = 144.8°, θ_3 = 123.1°, and θ_4 = 141.2°) suggests that Ala213 backbone atoms undergo significant fluctuations during the simulation time as opposed to the Glu211 backbone atoms and the side chain of Lys162.

Based on docking simulations, three hydrogen bonds were predicted for the compound **23**–Aurora A kinase complex. Among these hydrogen bonds (pyrazole ring NH···CO Ala213, sulfonamide NH···CO Asn261, and sulfonamide SO···NH_2 Lys162), two were preserved in approximately one third of the MD trajectory. The sulfonamide NH···CO Asn261 hydrogen bond appeared only in ~3% of the trajectory. Relatively low frequency of sulfonamide SO···NH_2 Lys162 hydrogen bond is due to the fact that Lys162 side chain evolved through significant conformational flexibility as evident from the transient hydrogen bonding interaction between the quinazoline N_1 and Lys162 side chain NH_2 function. All the predicted hydrogen bonds (except transient sulfonamide NH···CO Asn261 hydrogen bond) were restored in energy minimized average complex structure. It should be borne in mind that those atoms which lost the hydrogen bonding interaction during MD simulations could still be involved in electrostatic interactions.

Among the five hydrogen bonds (quinazoline N_1···NH Ala213, piperidine N···NH_2 Arg137, hydroxyl O···NH_2 Arg137, hydroxyl H···OH Tyr212, and benzamido NH···CO Ala273) between the compound **25**–Aurora A kinase complex, three were significantly preserved while remaining two were preserved only for approximately one quarter of the simulation time. The loss of hydrogen bond between benzamido –NH and –CO of Ala273 was compensated by the formation of a new hydrogen bond between the benzamido –CO and –NH_2 of Lys162 during the simulation time. MD simulations found a new hydrogen bond, formed between the pyrimidine N_1 and NH_2 of Lys162 with a living time of ~50% of the MD simulation. The loss of the hydrogen bond between the piperidine N and NH_2 of Arg137 was compensated by a two prong hydrogen bond between the hydroxyl O and NH_2 groups of Arg137. All the predicted hydrogen bonds (except for the quinazoline N_1···NH Ala213, hydroxyl H···OH Tyr212, and benzamido CONH···CO Ala273) were restored in energy minimized average complex structure. Two new hydrogen bonds (pyrimidine N_1···NH_2 Lys162 and benzamido CO···NH_2 Lys162) were seen in this complex structure. The benzamido carbonyl oxygen and Lys162 interaction was facilitated by a change in torsional angle defined by the pyrimidine N_1-pyrimidine C_2- and amide N–H was −20° in initial complex vs. −165° in the final average minimized complex. Thus a final complex is stabilized by a total of four hydrogen bonds instead of the original five predicted for a docked complex.

Based on the docking simulations, four hydrogen bonds were predicted in compound **27**–Aurora A kinase complex. Among the four hydrogen bonds (pyrazole ring N···NH Ala213, pyrazole ring NH···CO Ala213, CO···NH Phe144, and CO···NH Gly145), only two were reasonably preserved and the other two are regarded as transients during the MD simulation time. It is interesting to note that four new transient hydrogen bonds were seen during the simulation time and they could be responsible for the stabilization of the complex. A hydrogen bond that occurs with high frequency (CO···NH Gly145) was restored in the energy minimized average complex structure. The corresponding atoms involved in the missing hydrogen bonds as a result of conformational changes during MD simulation could still be engaged in electrostatic interactions.

All of the hydrogen bonds between the compound **28** and Aurora A kinase were found to be transient in nature during the simulation time. An additional hydrogen bond formed between –SO and NH_2 of Lys162 was preserved for approximately one third of the simulation time. Significant displacement of compound **28** was evident from the hydrogen bond formed between the indolinone ring –NH and the backbone of Ala213. All three predicted hydrogen bonds were restored in the energy-minimized average structure of the complex. A fourth new hydrogen bond (SO···NH_2 Lys162) was also observed in the structure of the inhibitor–enzyme complex.

Most of the transient hydrogen bonds detected during MD simulations were formed with amino acid residues located within the solvent-accessible region. The transient nature of such hydrogen bonds probably reflects the high conformational freedom of amino acids near the surface than that of amino acids buried into the hinge region.

No attempts were made to correlate biological activities with docking scores because the biological activity of compounds **9**–**23** have been reported as K_i of <100 nM. However, a detailed investigation of the binding modes of these inhibitors followed by MD simulations should serve as a useful tool for the future structure-based design of more potent and selective Aurora A kinase inhibitors.

3.6. Strategies to design further pyrazole and quinazoline derivatives active against Aurora A kinase

Our docking results provide a better understanding of the active site regions in Aurora A kinase that could be exploited as drug design targets. The presence of a *N*-methylpiperazine moiety of compounds **5**–**8** in the solvent-exposed front pocket warrants the placement of polar functions at this site to improve the pharmacokinetic profile of this class of compounds. Such modifications will be less likely to interfere with important inhibitor–active site residue interactions since they will be located outside the active site of Aurora A kinase. There is also an opportunity for modifying these compounds on the pyrazole nucleus (specifically at the C-6 carbon branching to turn the molecule from its original v-shape to a y-shape with a branching moiety forming a leg of the ''y'', *para*-substituted phenyl carboxamide group at one arm, a N-5 substituent at the

other arm and a tetrahydropyrrolo[3,4-*c*]pyrazole occupying the junction of two arms), as the selectivity (hydrophobic back) pocket is unoccupied by these compounds. Interestingly, this pocket is larger in Aurora A kinase than in other closely related kinases such as CDK-2 and Src [27]. Instead of Leu210 present in the selectivity pocket of Aurora A kinase; Src and CDK-2 have instead threonine and phenylalanine, respectively. As a result, whereas the phenylalanine (Phe80) in CDK-2 will restrict the size and entrance to the selectivity pocket, the threonine (Thr338) present in Src offers unique hydrogen bonding group and a less hydrophobic surface at the entrance to the selectivity pocket. Such differences in shape and charge of this pocket can be exploited for the design of most potent yet selective Aurora A kinase inhibitors.

Similarly, the C-6 and/or C-7 position of the quinazoline moiety in compounds **9**–**23** and the C-2 position of the quinazoline moiety and C-4 position of the pyrimidine ring in compound **25** could be modified with small hydrophobic groups such as $–CF_3$, –Cl, –F or $–CH_3$ to create additional binding contacts with and increase selectivity for the selectivity pocket of Aurora A kinase.

The information on recently synthesized pyrazole and quinazoline derivatives as Aurora A kinase inhibitors [13,15,16,25,28–30] along with the molecular docking/dynamics simulations described in this paper provide an excellent platform for rational design and development of potent and selective anticancer drugs. While this manuscript was nearing completion, several more potent and structurally diverse classes of Aurora A kinase inhibitors with defined K_i or IC_{50} values were synthesized in other laboratories [25,28–30]. We have started examining these new inhibitors using structure-based 3D-QSAR techniques and will be reporting the new results in a forthcoming communication.

4. Conclusions

We have developed a docking model for the tetrahydropyrrolo[3,4-*c*]pyrazole, quinazoline, pyrimidine and indolinone series of Aurora A kinase inhibitors. To the best of our knowledge, this is the first report on molecular docking and molecular dynamics on a recently resolved structure of Aurora A kinase. Glide 4.0, an automated docking program, successfully reproduced the binding mode of crystal structures (compounds **8** and **25**). The docking simulations suggested modifications to the pyrazole and the quinazoline series of Aurora A kinase inhibitors that may improve their inhibitory activity and selectivity, thus representing a valuable tool for the structure-based design of future pyrazole and quinazoline analogues. Four binding sites (A: solvent-exposed front pocket, B: hinge region, C: selectivity pocket and D: solvent-exposed phosphate binding region) seem to be required for the optimum binding of novel Aurora A kinase inhibitors. The MD simulations used here showed that complex formation between the inhibitors and Aurora A kinase did not alter the enzyme structure to a significant extent. The predicted hydrogen bonds between the Aurora A kinase and the inhibitors were restored in the energy minimized average structure of the complex.

Acknowledgements

TT wishes to thank Dean Robert Mangione and Dr. Louis Trombetta for providing start-up funds to purchase Schrodinger software package. We thank Drs. V. Hariprasad and Cesar Lau-Cam for helpful comments and suggestions. The authors also thank Mr. Pallav Patel and Shridhar Kulkarni for their help in preparing Fig. 5.

References

[1] P. Meraldi, R. Honda, E.A. Nigg, Curr. Opin. Genet. Dev. 14 (2004) 29.
[2] T. Tanaka, M. Kimura, K. Matsunaga, D. Fukada, H. Mori, Y. Okano, Cancer Res. 59 (1999) 2041.
[3] J.R. Bischoff, et al. EMBO J. 17 (1998) 3052.
[4] S. Sen, H. Zhou, R.A. White, Oncogene 14 (1997) 2195.
[5] S.L. Warner, D.J. Bearss, H. Han, D.D. Von Hoff, Mol. Cancer Ther. 2 (2003) 589.
[6] M. Kimura, S. Kotani, T. Hattori, S. Noriko, T. Yoshioka, K. Todokoro, Y. Okano, J. Biol. Chem. 272 (1997) 13766.
[7] H. Katayama, W.R. Brinkley, S. Sen, Cancer Metastasis Rev. 22 (2003) 451.
[8] H. Katayama, K. Sasai, H. Kawai, Z.M. Yuan, J. Bondaruk, F. Suzuki, S. Fujii, R.B. Arlinghaus, B.A. Czerniak, S. Sen, Nat. Genet. 36 (2004) 55.
[9] B.J. Druker, et al. N. Eng. J. Med. 344 (2001) 1031.
[10] A. Onn, M. Tsuboi, N. Thatcher, Br. J. Cancer 91 (2004) S11.
[11] E.A. Harrington, et al. Nat. Med. 10 (2004) 262.
[12] C. Garcia-Echeverria, P. Traxler, D.B. Evans, Med. Res. Rev. 20 (2000) 28.
[13] D. Fancelli, et al. J. Med. Chem. 48 (2005) 3080.
[14] D. Bebbington, J. Charrier, J. Golec, A. Miller, R. Knegtel, United States Patent Application US 2005/038023 (2005).
[15] F.H. Jung, et al. J. Med. Chem. 49 (2006) 955.
[16] N.M. Heron, et al. Bioorg. Med. Chem. Lett. 16 (2006) 1320.
[17] S. Hauf, R.W. Cole, S. LaTerra, C. Zimmer, G. Schnapp, R. Walter, A. Heckel, J. van Meel, C.L. Rieder, J. Peters, J. Cell Biol. 161 (2003) 281.
[18] C. Ditchfield, V.L. Johnson, A. Tighe, R. Ellston, C. Haworth, T. Johnson, A. Mortlock, N. Keen, S.S. Taylor, J. Cell Biol. 161 (2003) 267.
[19] W.L. Jorgensen, D. Maxwell, J. Tirado-Rives, J. Am. Chem. Soc. 118 (1996) 11225.
[20] I. Bytheway, S. Cochran, J. Med. Chem. 47 (2004) 1683.
[21] H. Chen, P.D. Lyne, F. Giordanetto, T. Lovell, J. Li, J. Chem. Inf. Model. 46 (2006) 401.
[22] R.A. Friesner, et al. J. Med. Chem. 47 (2004) 1739.
[23] T.A. Halgren, R.B. Murphy, R.A. Friesner, H.S. Beard, L.L. Frye, W.T. Pollard, J.L. Banks, J. Med. Chem. 47 (2004) 1750.
[24] M.D. Eldridge, C.W. Murray, T.R. Auton, G.V. Paolini, R.P. Mee, J. Comput. -Aided Mol. Des. 11 (1997) 425.
[25] K.J. Moriarty, et al. Bioorg. Med. Chem. Lett. 16 (2006) 5778.
[26] F. Sessa, M. Mapelli, C. Ciferri, C. Tarricone, L.B. Areces, T.R. Schneider, P.T. Stukenberg, A. Musacchio, Mol. Cell 18 (2005) 379.
[27] G.M.T. Cheetham, R.M.A. Knegtel, J.T. Coll, S.B. Renwick, L. Swenson, P. Weber, J.A. Lippke, D.A. Austen, J. Biol. Chem. 277 (2002) 42419.
[28] D. Fancelli, et al. J. Med. Chem. 49 (2006) 7247.
[29] A.A. Mortlock, et al. J. Med. Chem. 50 (2007) 2213.
[30] L.W. Tari, I.D. Hoffman, D.C. Bensen, M.J. Hunter, J. Nix, K.J. Nelson, D.E. McRee, R.V. Swanson, Bioorg. Med. Chem. Lett. 17 (2007) 688.